IMMUNOLOGY

The making of a nucleic acid sensor at the dawn of jawed vertebrate evolution

Zhiwei Wu, Lingyu Chu, Zhen Gong, Guan-Zhu Han*

Self and nonself discrimination is fundamental to immunity. However, it remains largely enigmatic how the mechanisms of distinguishing nonself from self originated. As an intracellular nucleic acid sensor, protein kinase R (PKR) recognizes double-stranded RNA (dsRNA) and represents a crucial component of antiviral innate immunity. Here, we combine phylogenomic and functional analyses to show that PKR proteins probably originated from a preexisting kinase protein through acquiring dsRNA binding domains at least before the last common ancestor of jawed vertebrates during or before the Silurian period. The function of PKR appears to be conserved across jawed vertebrates. Moreover, we repurpose a protein closely related to PKR proteins into a putative dsRNA sensor, recapturing the making of PKR. Our study illustrates how a nucleic acid sensor might have originated via molecular tinkering with preexisting proteins and provides insights into the origins of innate immunity.

INTRODUCTION

Distinguishing self and nonself is an essential prerequisite for innate immunity. Innate immune systems use an array of pattern recognition receptors (PRRs) to detect pathogen infection. PRRs recognize molecular structures as characteristic of pathogens which is known as microbe- or pathogen-associated molecular patterns (MAMPs or PAMPs), allowing the host to discriminate nonself from self (*1*, *2*). Nucleic acids are a major class of PAMPs recognized by PRRs that are collectively termed as nucleic acid sensors (*1*, *2*).

Virus infection produces double-stranded RNA (dsRNA) (*1*, *2*). Immune responses to viral infection can be activated by the recognition of dsRNA by a set of dsRNA sensors, such as protein kinase R (PKR), RIG-1–like receptors, Toll-like receptor 3 (TLR3), 2′-5′-oligoadenylate synthetase 1 (OAS1), adenosine deaminase acting on RNA 1, and NOD-, LRR- and pyrin domain–containing 1 (NLRP1) (*1*, *2*). Notably, dsRNA can be also produced from endogenous sources upon dysregulated cellular processes, often serving as a danger signal (*3*).

PKR is among one of the first identified nucleic acid sensors (*4*). PKR and other related kinases, such as heme-regulated inhibitor kinase (HRI), the unfolded protein response regulator PKR-like endoplasmic reticulum kinase (PERK), and the metabolite sensor general control nonderepressible-2 (GCN2), share the ability to phosphorylate the α subunit of eukaryotic initiation factor 2 (eIF2α) on the same regulatory site, Ser^{51}, in response to various cellular stresses (*5*–*7*). Upon the binding of dsRNA, PKR dimerizes and autophosphorylates, leading to the full catalytic activation of PKR. Activated PKR then phosphorylates eIF2α, converting eIF2α into an inhibitor of its guanine nucleotide exchange factor eIF2B and thereby downregulating translation (Fig. 1A) (*6*, *7*). The activity of PKR causes a general reduction in protein synthesis and thus blocks viral replication (*6*, *7*). PKR represents a crucial component of antiviral innate immunity (*8*–*11*).

The conflict between hosts and pathogens leads to recurrent evolutionary arms race, exerting positive selection on the genes from both sides involved (*12*–*14*). Viruses have evolved diverse countermeasures to antagonize the function of PKR proteins (*15*). For instance, poxviruses encode a mimic of eIF2α called K3L, and K3L functions as a pseudo-substrate for PKR (*15*–*17*). To be effective, PKR evolves to keep recognizing eIF2α and, in the meanwhile, to escape the rapidly evolving mimic K3L (*18*). The *PKR* gene is subject to intensive episodic positive selection in primates (*7*, *18*).

In this study, we combined phylogenomic and functional analyses to interrogate the origin and evolution of PKR proteins. We found that PKR proteins are likely to have originated from a preexisting eIF2α kinase through gaining dsRNA binding domains (dsRBDs) before the last common ancestor (LCA) of jawed vertebrates and probably after the divergence of jawed and jawless vertebrates. The function of PKR is conserved across jawed vertebrates. Our study illustrates how a nucleic acid sensor originated via molecular tinkering at the dawn of jawed vertebrate evolution.

RESULTS

The origin of PKR proteins before the LCA of jawed vertebrates

The human PKR protein (hsPKR; hs indicates the species source, *Homo sapiens*) consists of two tandem dsRBDs (accession: pfam00035) and a kinase domain (accession: cl21453) (Fig. 1B). To interrogate the origin of PKR proteins, we first analyzed the distribution and evolutionary relationship of kinase domains across 246 representative cellular organisms, including 21 bacteria, 15 archaea, and 210 eukaryotes, 154 of which are metazoans (table S1). Mediating diverse crucial biological function, kinase-containing proteins are ubiquitously distributed across cellular organisms. Large-scale phylogenetic analyses of kinase domains show that hsPKR clusters within the diversity of a group of serine/threonine kinase proteins collectively known as eIF2α kinases (EIF2AKs) (Fig. 1C and fig. S1). The EIF2AK group also includes HRI, GCN2, and PERK. Next, we performed further phylogenomic analyses of EIF2AK proteins (table S2). Our phylogenetic analyses show that kinase-encoding proteins with dsRBDs cluster together with strong support, which is designated the PKR group hereafter, and PKZ (protein kinase containing Z-DNA binding domains) proteins nest within the diversity

College of Life Sciences, Nanjing Normal University, Nanjing, Jiangsu 210023, China.
*Corresponding author. Email: guanzhu@njnu.edu.cn

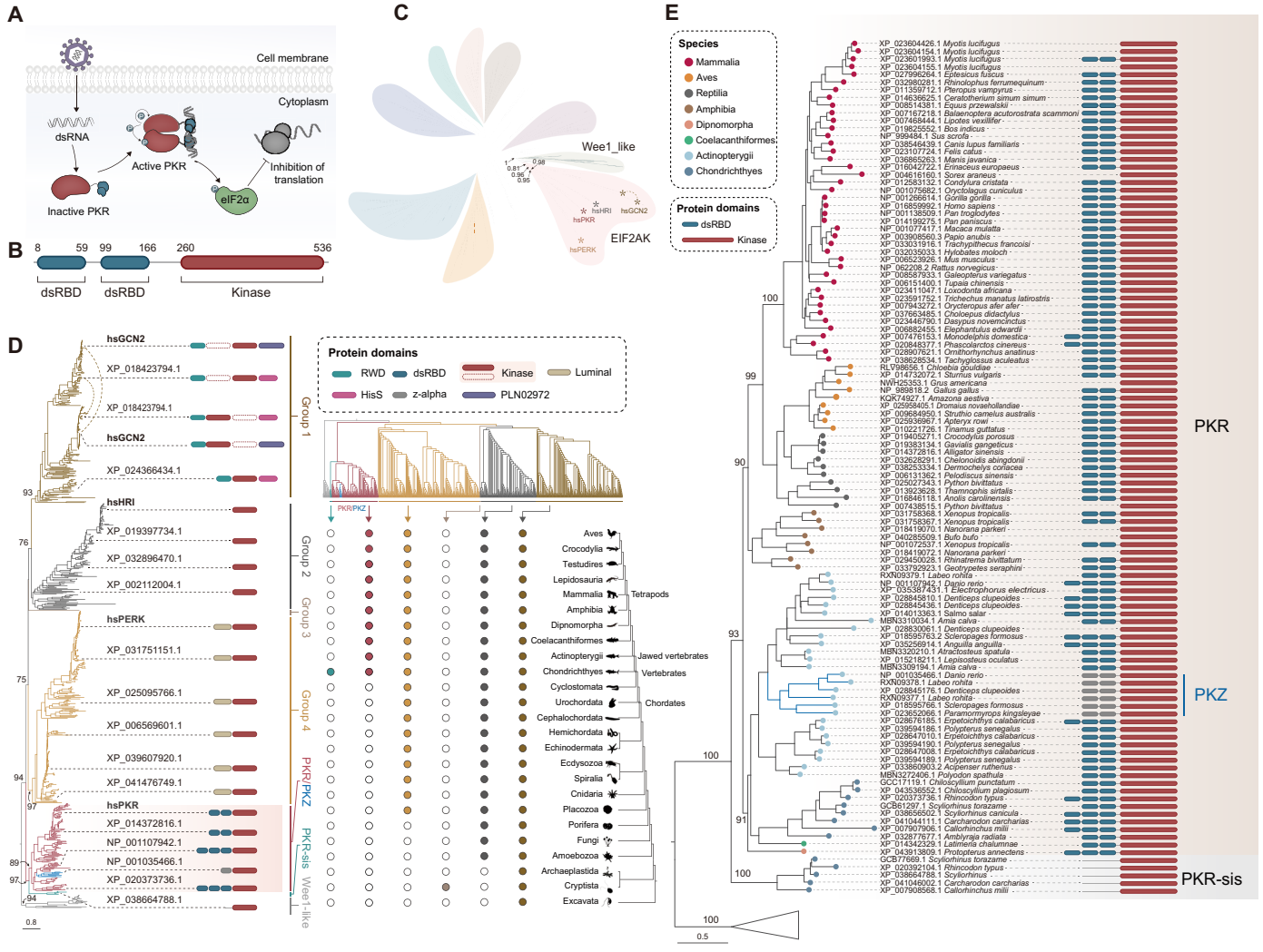

Fig. 1. Phylogenetic analyses of PKR related proteins. (**A**) Model for PKR-mediated antiviral innate immunity. Upon recognition of dsRNA produced by virus infection, PKR dimerizes and autophosphorylates, leading to the full catalytic activation of PKR. Activated PKR then phosphorylates eIF2α, converting eIF2α into an inhibitor of its guanine nucleotide exchange factor eIF2B and thereby down-regulating translation. (**B**) The domain architecture of hsPKR (accession: NP_002750.1). hsPKR consists of two tandem dsRBDs and a kinase domain. The numbers indicate the start or termination sites for different domains. (**C**) Large-scale phylogenetic analyses of PKR homologs based on the kinase domain sequences. Major kinase clades are marked in different colors. For more detailed information, see also fig. S1. Support values are shown near the selected nodes. (**D**) Phylogenetic analysis of EIF2AK proteins based on the kinase domain sequences (accession: cl21453) with Wee1-like kinases as the outgroup. The PKR protein group was highlighted in red. Domain architectures of representative proteins are shown. For proteins with more than one kinase domains, kinase domains were partitioned and analyzed independently, and kinase domains analyzed are labeled with solid red rectangles. The distribution for different EIF2AK groups in cellular organisms is shown, and filled and empty circles indicate the presence and absence of corresponding EIF2AK group proteins, respectively. Support values are shown near the selected nodes. (**E**) Phylogenetic relationships of proteins closely related to PKR proteins based on the kinase domain sequences (accession: cl21453). For each protein, domain architecture is shown. Support values are shown near the selected nodes.

of the PKR group (Fig. 1D). The PKR group proteins are present in all the major lineages of jawed vertebrates but not present in species outside jawed vertebrates. We found that a group of kinase-encoding proteins without dsRBD from cartilaginous fishes are sister to the PKR group proteins and are thus termed as PKR-sis proteins (Fig. 1E). Both PKR group and PKR-sis proteins share significant structural similarity to the hsPKR protein (fig. S2). Together, our phylogenomic analyses suggest that PKR proteins might have originated from a preexisting EIF2AK protein that can phosphorylate eIF2α through acquiring dsRBDs at least before the LCA of modern jawed vertebrates and probably after the divergence of jawed and jawless vertebrates during or before the Silurian period (444 to 419 million years ago) (*19*, *20*).

The origin and evolution of dsRBD in PKR proteins

To elucidate the origin of dsRBDs in PKR proteins, we performed phylogenomic analyses of dsRBD-encoding proteins across cellular organisms (table S1). Most of PKR proteins encode at least two tandem dsRBDs. Our phylogenetic analyses of dsRBDs show that the two dsRBDs of PKR proteins cluster together but form two distinct subgroups, namely, PKR-1 and PKR-2 (Fig. 2). Both PKR-1 and PKR-2 dsRBDs are present in PKR proteins across jawed vertebrates

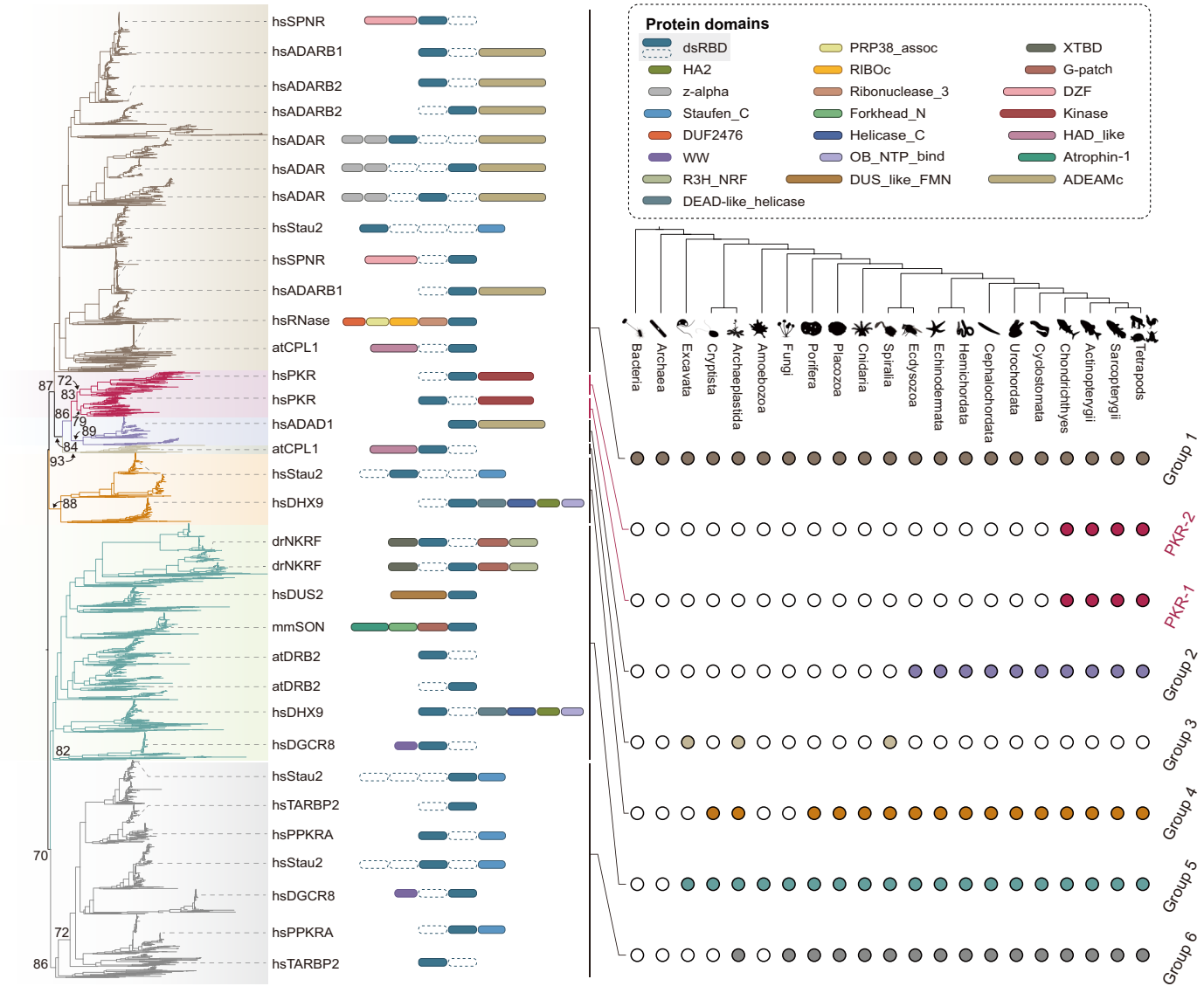

Fig. 2. Phylogenetic analysis of dsRBD-containing proteins. Phylogenetic analyses of diverse dsRBD-containing proteins were performed based on the dsRBD sequences. Domain architectures of representative proteins were shown. For proteins with more than one dsRBDs, dsRBDs were partitioned and analyzed independently, and dsRBDs analyzed are labeled with solid blue rectangles. The distribution for different dsRBD groups is shown on the right. Filled and empty circles indicate the presence and absence of corresponding dsRBD group proteins, respectively.

(Fig. 2). These results suggest that the two tandem dsRBDs in PKR proteins might have arisen through an ancient duplication after the progenitor EIF2AK acquired a single dsRBD likely before the LCA of jawed vertebrates (Fig. 2). Furthermore, we also found lineage-specific duplication of dsRBDs occurred during the evolution of PKR proteins in jawed vertebrates, generating PKR proteins with three or more dsRBDs. The dsRBDs from PKR proteins are closely related with those from adenosine deaminase domain containing 1 (ADAD1) and C-terminal domain phosphatase-like 1 (CPL1) proteins, but it remains uncertain where PKR proteins gained its dsRBD (Fig. 2). Nevertheless, it should be noted that dsRBD sequence is short in length, and thus phylogenetic analysis of dsRBD sequences should be taken with caution as indicated by intermediate support values.

Conserved function of PKR proteins across jawed vertebrates

To test whether the function of PKR proteins is conserved across jawed vertebrates, we used a proven budding yeast (*Saccharomyces cerevisiae*) model (*7*, *21*, *22*). Budding yeast constitutively produces dsRNA in the cytosol (*22*–*24*). hsPKR can recognize and phosphorylate yeast eIF2α. Consistent with previous studies (*7*, *21*, *22*), we found that expression of hsPKR with a galactose-inducible promoter inhibited yeast cell growth (Fig. 3A). We examined the phosphorylation status of eIF2α using antibodies specific for eIF2α phosphoserine-51 and observed the phosphorylation of eIF2α. We introduced a mutation, K296A, in the catalytic subdomain II of hsPKR, which can disrupt the kinase activity of hsPKR (*25*). The expression of hsPKR^{K296A} did not impair yeast growth, and no

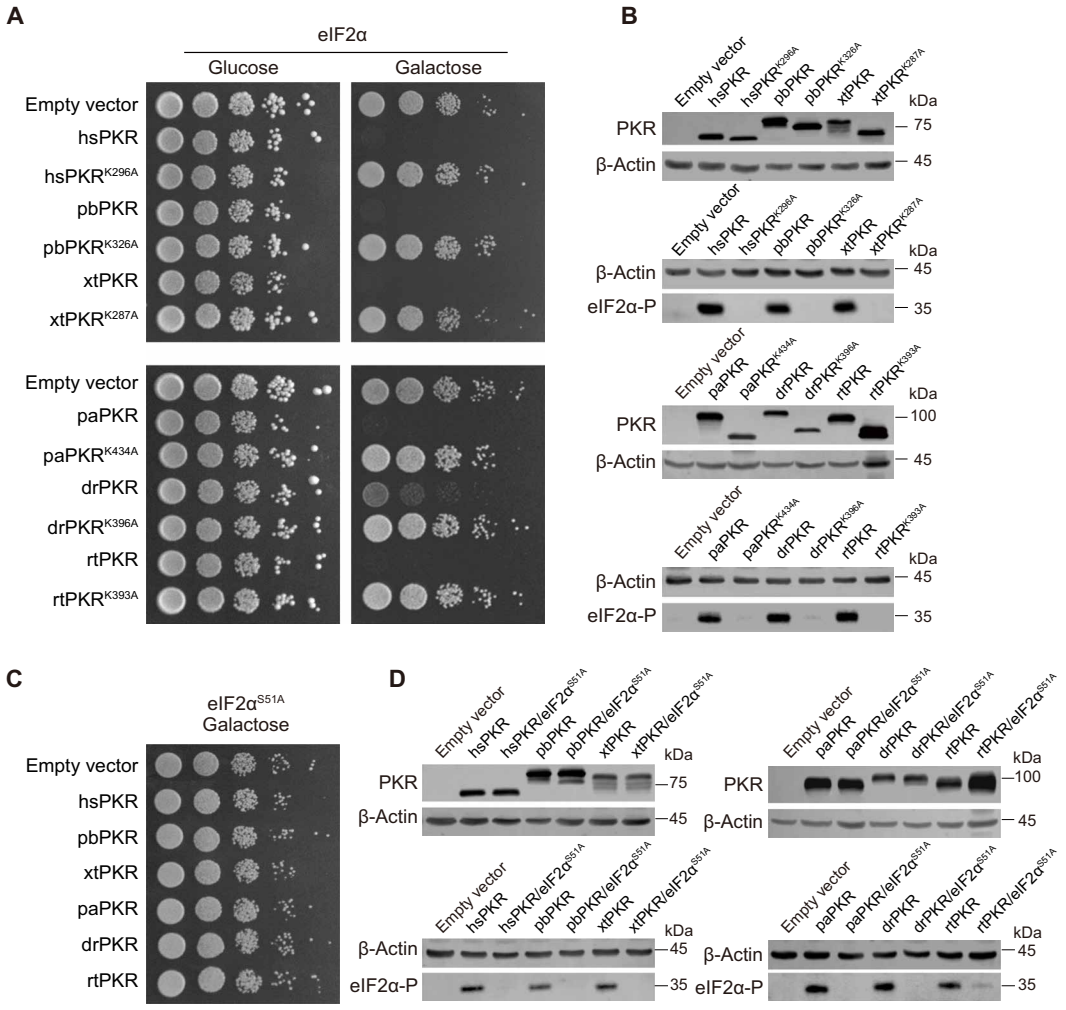

Fig. 3. Functional analyses of PKR proteins in the yeast system. Functional analyses of *PKR* genes from six representative jawed vertebrates, namely, *hsPKR* of *H. sapiens*, *pbPKR* of *P. bivittatus*, *xtPKR* of *X. tropicalis*, *paPKR* of *P. annectens*, *drPKR* of *D. rerio*, and *rtPKR* of *R. typus*, were performed in the yeast system. (**A**) Transformation of wild-type yeast strains with plasmids expressing *PKR* genes or *PKR* genes with kinase-dead mutations under the control of a galactose-inducible promoter. After a series of 10-fold dilutions, the transformants were spotted on the surface of solid medium containing glucose or galactose and incubated at 30°C for 48 or 72 hours, respectively. (**B**) Whole-cell extracts from transformants were separated by 10% SDS-PAGE gel and detected by Western blotting with antibodies against HA tag, β-actin, and phospho-specific antibodies against Ser^{51} in eIF2α (eIF2α-P), respectively. (**C**) Transformation of $eIF2\alpha^{S51A}$ strains with plasmids expressing *PKR* genes under the control of a galactose-inducible promoter. After a series of 10-fold dilutions, the transformants were spotted on the surface of solid medium containing galactose and incubated at 30°C for 72 hours. (**D**) Whole-cell extracts from transformants were separated by 10% SDS-PAGE gel and detected by Western blotting with antibodies against HA tag and β-actin, as well as phosphospecific antibodies against Ser^{51} in eIF2α (eIF2α-P), respectively.

phosphorylation of eIF2α was observed. Moreover, we constructed a yeast strain with a nonphosphorylatable mutation, S51A, in eIF2α. In the yeast strain with $eIF2\alpha^{S51A}$, the expression of hsPKR did not inhibit the yeast growth, and no phosphorylation of eIF2α was observed. Therefore, these results confirm that the yeast system represents an efficient platform to study the function of PKR proteins (*7*, *21*, *22*).

Then, we expressed *PKR* genes from five additional species that cover the diversity of jawed vertebrates in yeast, including *pbPKR* from the Burmese python *Python bivittatus* (a reptile), *xtPKR* from the western clawed frog *Xenopus tropicalis* (an amphibian), *paPKR* from the African lungfish *Protopterus annectens* (a lobe-finned fish), *drPKR* from the zebrafish *Danio rerio* (a ray-finned fish), and *rtPKR* from the whale shark *Rhincodon typus* (a cartilaginous fish). The expression of all the five *PKR* genes attenuated the yeast cell growth, and eIF2α proteins were phosphorylated (Fig. 3B). When introducing the kinase-dead mutations corresponding to K296A in hsPKR into these five *PKR* genes, no impaired yeast growth and no eIF2α phosphorylation were observed (Fig. 3B). Consistently, these five PKR proteins were not phosphorylated as indicated by their downward shifts in SDS–polyacrylamide gel electrophoresis (PAGE) gel migration (Fig. 3B). When these five *PKR* genes were expressed in the yeast strain with $eIF2\alpha^{S51A}$, no impaired yeast growth and no eIF2α phosphorylation was observed (Fig. 3, C and D). Together, these results suggest that the function of PKR is well conserved across jawed vertebrates.

Repurposing an EIF2AK protein into a dsRNA sensor

We identified a group of kinase proteins (dubbed PKR-sis proteins) that are sister to PKR proteins in cartilaginous fishes (Fig. 1D). PKR-sis proteins only encode kinase domains but no dsRBD (Fig. 1D). When we expressed the PKR-sis protein of the small-spotted catshark *Scyliorhinus canicula* (scPKR-sis) in yeast, yeast appears to grow normally (Fig. 4, A and B). To examine the requirement of dimerization for PKR-sis activity, we fused full-length scPKR-sis and the kinase domain (residues 260 to 537) of scPKR-sis (scPKR-sis-KD) to glutathione *S*-transferase (GST), which can form homodimers. The expression of GST-scPKR-sis and GST-scPKR-sis-KD resulted in yeast growth arrest and the phosphorylation of eIF2α. When expressing GST-scPKR-sis and GST-scPKR-sis-KD with a kinase-dead mutation, K294A, no yeast growth impairment and reduced eIF2α phosphorylation was observed (Fig. 4, A and B). These results suggest that like PKR proteins, dimerization is required for the activity of scPKR-sis. We also expressed GST-scPKR-sis and GST-scPKR-sis-KD in the yeast strain with eIF2α^{S51A}, but no impaired yeast growth and no phosphorylation of eIF2α was observed (Fig. 4, C and D), suggesting that scPKR-sis is an EIF2AK.

To test whether PKR-sis can readily act as a dsRNA sensor by gaining dsRBDs, we grafted the two dsRBDs (residues 1 to 259) of hsPKR on the kinase domain of scPKR-sis, which is designated chimeric PKR 1 (cPKR1). However, the expression of cPKR1 did not inhibit the growth of yeast (Fig. 5, A to C). Then, we replaced a 123-residue region within cPKR1 with the corresponding region (residues 260 to 382) of the kinase domain of hsPKR, generating cPKR2. The expression of cPKR2 impaired the growth of yeast, and enhanced eIF2α phosphorylation was observed (Fig. 5, A to C). However, replacing two smaller regions of cPKR1 with the corresponding regions of hsPKR (residues 260 to 320 or residues 321 to 382) did not inhibit yeast growth, indicating that certain residues in the two smaller regions work together to impair yeast growth (Fig. 5, A to C). To identify the crucial residues, we constructed a series of chimeric proteins and narrowed down the functionally relevant regions to residues 275 to 289 and residues 354 to 368 (Fig. 5, D to G). Comparative analysis of PKR and PKR-sis protein sequences show that two residues (Lys^{283} and Phe^{363} in hsPKR; Glu^{281} and Cys^{342} in scPKR-sis) within the functionally relevant regions identified above are conserved among PKR proteins but differ between PKR and PKR-sis proteins (fig. S3). Thus, we

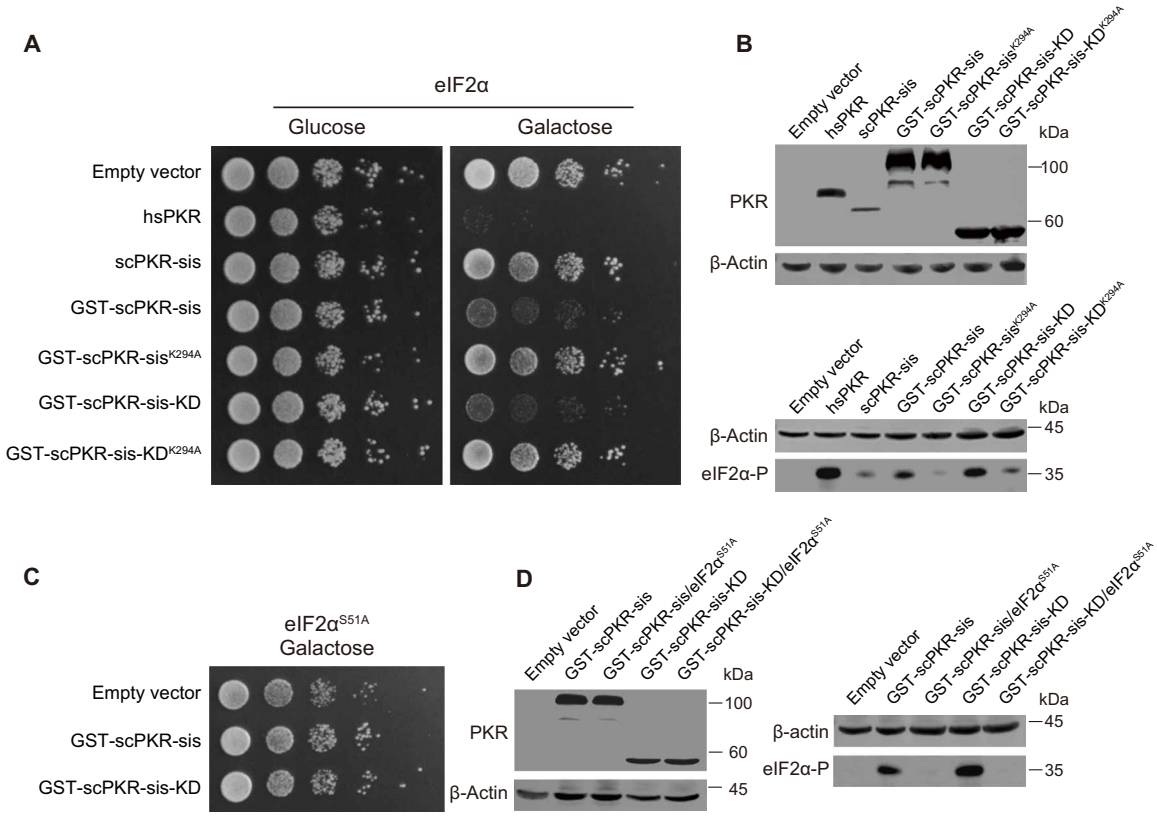

Fig. 4. Functional analyses of PKR-sis proteins in the yeast system. Functional analyses of *scPKR-sis* gene were performed in the yeast system. (**A**) Transformation of wild-type yeast strains with plasmids expressing GST-scPKR-sis and GST-scPKR-sis-KD fusion proteins or GST-scPKR-sis and GST-scPKR-sis-KD fusion proteins with kinase-dead mutations under the control of a galactose-inducible promoter. Yeast transformants were subjected to 10-fold serial dilution and tested for growth on solid medium containing glucose or galactose. (**B**) Whole-cell extracts from transformants were separated by 10% SDS-PAGE gel and detected by Western blotting with antibodies against HA tag, GST tag, and β-actin, as well as phosphospecific antibodies against Ser^{51} in eIF2α (eIF2α-P), respectively. (**C**) Plasmids expressing GST-scPKR-sis and GST-scPKR-sis-KD fusion protein under the control of a galactose-inducible promoter were introduced into yeast strain S288C containing eIF2α^{S51A}. Transformants were subjected to 10-fold serial dilution and tested for growth on solid medium containing glucose or galactose. (**D**) Whole-cell extracts from transformants were separated by 10% SDS-PAGE gel and detected by Western blotting with antibodies against GST tag and β-actin, as well as phosphospecific antibodies against Ser^{51} in eIF2α (eIF2α-P), respectively.

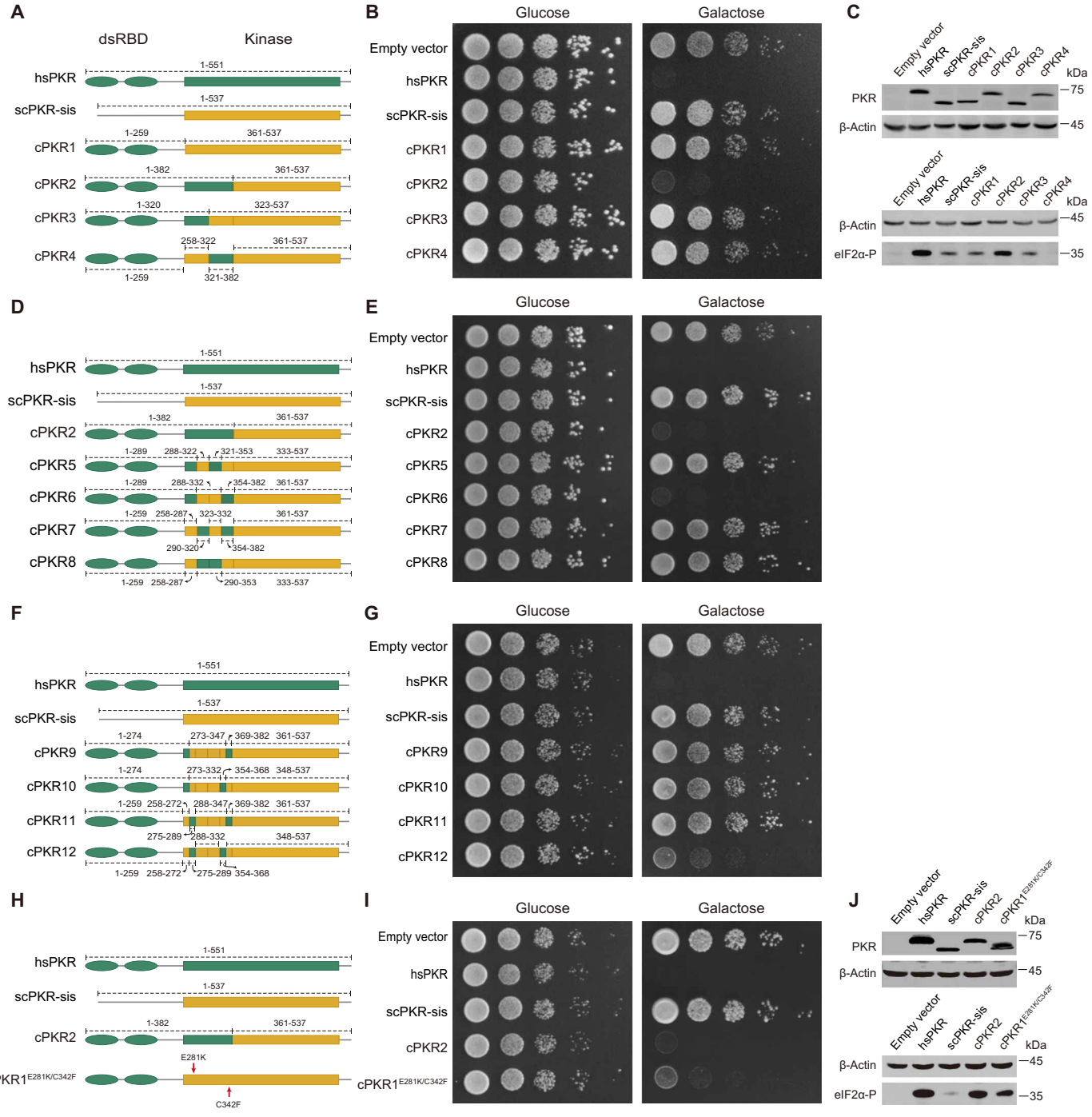

Fig. 5. Repurposing an EIF2AK protein into a putative dsRNA sensor. (**A**, **D**, **F**, and **H**) Schematic diagram of chimeric PKR construction. Chimeric PKR proteins, cPKR1 to cPKR4, are derived from hsPKR and scPKR-sis. Sequence fragments from different sources are indicated using different colors. The numbers indicate the corresponding sites in source proteins. (**B**, **E**, **G** and **I**) Functional analysis of hsPKR, scPKR-sis, and chimeric PKR proteins in the yeast system. Transformation of wild-type yeast strains with plasmids expressing *hsPKR*, *scPKR-sis*, and chimeric *PKR* genes under the control of a galactose-inducible promoter. After a series of 10-fold dilutions, the transformants were spotted on the surface of solid medium containing glucose or galactose and incubated at 30°C for 48 or 72 hours, respectively. (**C** and **J**) Western blot analysis was used to detect the expression of corresponding proteins and the phosphorylation of eIF2α. Whole-cell extracts from transformants were separated by 10% SDS-PAGE gel and detected by Western blotting with antibodies against HA tag and β-actin, as well as phosphospecific antibodies against Ser51 in eIF2α (eIF2α-P), respectively.

introduced two mutations corresponding to the two residues, E281K and C342F, to cPKR1. The expression of cPKR1$^{E281K/C342F}$ resulted in attenuated yeast growth and enhanced phosphorylation of eIF2α (Fig. 5, H to I). The two residues are well conserved among PKR proteins, but not among EIF2AK proteins (fig. S3). Together, our results show that a cartilaginous fish PKR-sis protein can be repurposed into a putative dsRNA sensor by gaining dsRBDs and modifying two residues.

DISCUSSION

In this study, we combined phylogenomic and functional analysis approaches to dissect the origin and evolution of the dsRNA sensor PKR. Our results suggest that PKR is likely to have originated from a preexisting kinase protein by gaining dsRBDs at least before the LCA of modern jawed vertebrates and after the divergence of jawed and jawless vertebrates during or before the Silurian period (444 to 419 million years ago) (Fig. 6) (*19*, *20*). The function of PKR proteins appears to be conserved across jawed vertebrates. Our study provides insights into the origins and evolution of innate immune systems.

PKR consists of a kinase domain and typically two tandem dsRBD repeats. On one hand, PKR, HRI, PERK, and GCN2 share a common kinase domain that specifically phosphorylates Ser^{51} on eIF2α, but each of them has unique regulatory domains (*5*–*7*). Different regulatory domains enable them to respond to different stresses (PKR to viral infection, HRI to heme deficiency, PERK to endoplasmic reticulum stress, and GCN2 to amino acid limitation) (*5*–*7*). Our results show that scPKR-sis is also an EIF2AK. Phylogenetic analyses of kinase domains show that PKR, PKR-sis, HRI, PERK, and GCN2 proteins cluster into a group (Fig. 1, C and D). It is conceivable that the common function of this protein group is likely to phosphorylate eIF2α. Therefore, PKR proteins are likely to have originated from a progenitor that can phosphorylate Ser^{51} on eIF2α (Fig. 6). On the other hand, dsRBDs recognize dsRNA and are present in diverse proteins implemented in innate immunity and cellular dsRNA homeostasis, such as ADAD1 and Staufen, across cellular organisms. Phylogenetic analyses indicate that the two tandem dsRBDs of PKR proteins might be generated by duplication after the EIF2AK progenitor acquired a single dsRBD before the LCA of jawed vertebrates (Fig. 6), albeit with caution due to the short nature of dsRBD sequences. We repurposed a PKR-sis protein into a putative dsRNA sensor through dsRBD graft and mutations in two residues, which recaptures the making of PKR proteins. Therefore, our results indicate that PKR proteins originated through molecular tinkering with preexisting proteins (Fig. 6). Moreover, PKZ might function as a Z-DNA/Z-RNA sensor to activate immune responses (*26*–*28*). Our phylogenetic analysis shows that PKZ proteins nest within the diversity of PKR proteins from ray-finned fishes, suggesting that PKZ proteins might have originated from PKR proteins via the replacement of dsRBDs by Z-DNA binding domains during the evolutionary course of ray-finned fishes (Fig. 1D). Together, this study reemphasizes the significance of molecular tinkering in the origins of innate immune systems, as revealed by the cases of the

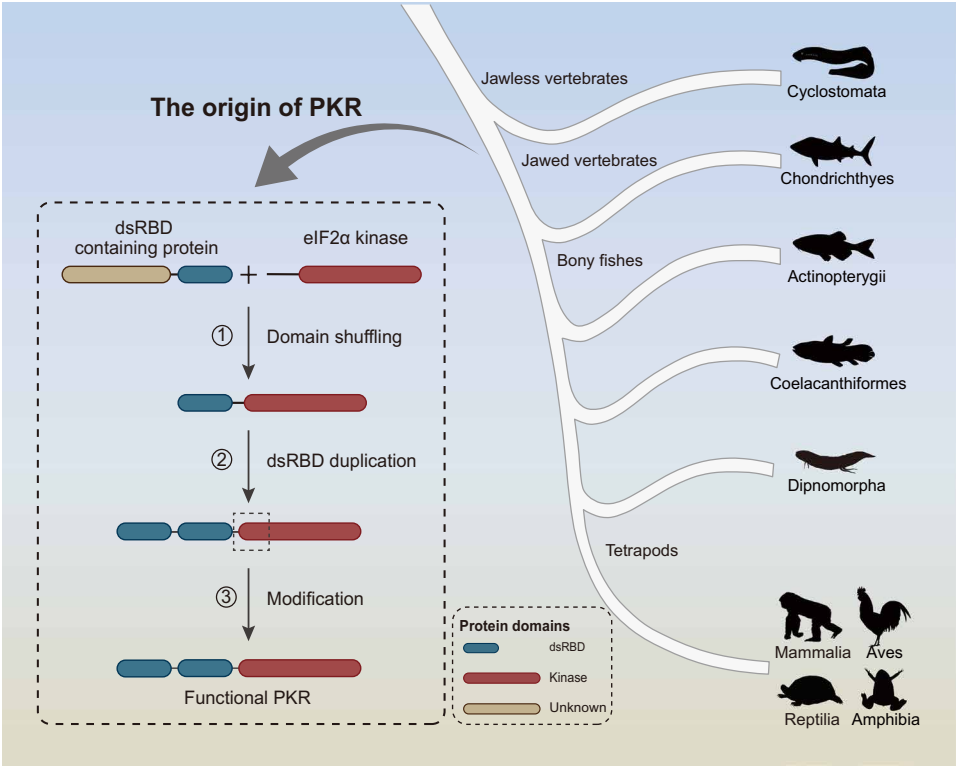

Fig. 6. Evolutionary scenarios for the making of PKR proteins. PKR proteins probably originated before the LCA of jawed vertebrates, but after the divergence of jawless and jawed vertebrates. Domain shuffling occurred between a dsRBD-containing protein and a preexisting EIF2AK protein that can phosphorylate eIF2α, giving rise to the PKR progenitor. dsRBD duplication and further modifications occurred in the progenitor, generating the functional PKR. The function of PKR is conserved across jawed vertebrates.

HOPZ-ACTIVATED RESISTANCE 1 resistosome in angiosperms (*29*) and the OAS–ribonuclease L (RNase L) pathways in vertebrates (*30*).

Our previous study shows that the OAS–RNase L innate immune pathway that also senses dsRNA as nonself likely originated before the rise of jawed vertebrates (*30*). The two dsRNA sensing mechanisms, PKR proteins and the OAS–RNase L pathway, and the so-called "Big Bang" of adaptive immunity (*31*–*34*) are likely to have arisen within the same time interval, namely, before the LCA of modern jawed vertebrates and after the divergence between jawed and jawless vertebrates. However, other innate immune mechanisms originated at other times (*35*), for instance, (i) canonical TLRs, PRRs on cell surfaces sensing PAMPs, have been thought to be distributed in eumetazoans and might thus have originated during the early evolution of eumetazoans (*36*, *37*). However, TIR domains seem to have a much earlier origin and are also widely distributed in plants and bacteria (*38*). It has been hypothesized that TLRs emerged from molecular tinkering with TIR domain– and LRR domain–containing proteins. (ii) For the cyclic guanosine 3′,5′-monophosphate–adenosine 3′,5′-monophosphate synthase (cGAS) stimulator of interferon genes (STING) pathway, cGAS-like receptors (cGLRs) constitute a major family of PRRs that recognize double-stranded DNA and dsRNA and are present in nearly all the metazoan phyla (*39*, *40*). cGLRs probably originated from horizontal gene transfer (HGT) from bacteria (*40*). Canonical STING proteins from metazoans share distant homolog with STING effectors of cyclic oligonucleotide-based antiphage signaling system of bacteria (*41*). STING-like proteins are also present in other eukaryotes, such as amoebozoans and choanoflagellates (*40*). (iii) Although the canonical OAS–RNase L pathway originated before the LCA of jawed vertebrates, OAS-like proteins are more widely distributed in metazoans, amoebozoans, and choanoflagellates, and might have also arisen through HGT from bacteria (*30*, *40*). (iv) Viperin catalyzes the conversion of cytidine triphosphate (CTP) to 3′-deoxy-3′,4′-didehydro–CTP that acts as a chain terminator for viral RNA–dependent RNA polymerases and thus inhibits viral replication (*42*). Viperins are widely present in cellular organisms, and viperins from prokaryotes produce a set of modified ribonucleotides and can thwart phage infections (*43*). It follows that the origin of viperin proteins might have a deep root in the early evolution of cellular organisms. Together, we can conclude that the arsenal of innate immunity has been endlessly supplemented and modified during the evolution of life.

MATERIALS AND METHODS

Identification of PKR proteins

We used a similarity search and phylogenetic analysis combined approach to identify PKR homologs in 246 representative species that cover the major diversity of cellular organisms, including 21 bacteria, 15 archaea, and 210 eukaryotes, 154 of which are metazoans. To identify PKR homologs, we used the BLASTP or TBLASTN algorithms to search against the proteomes or genomes of cellular organisms with kinase domain sequences (accession: cl21453) as queries and an *e*-cutoff value of 10^{-5}. To identify dsRBD homologs, we used the HMMER (*44*) algorithm to search against the proteomes of cellular organisms. All the significant hits were aligned using the MAFFT version 7.0 (*45*) and refined manually. Large-scale phylogenetic analyses were performed using an approximate maximum likelihood method implemented in FastTree version 2.1.9 (*46*). Sequences that cluster with PKR proteins (including PKZ proteins) were retrieved, and phylogenetic analysis was performed using a maximum likelihood method implemented in IQ-TREE version 2.0 (*47*). The domain architectures were annotated using CD-search (*48*). The structures of representative PKRs were predicted using ColabFold version 1.5.2 (*49*) or AlphaFold (*50*). PKR protein structure similarity was compared using the pairwise structure alignment strategy from Research Collaboratory for Structural Bioinformatics protein database (*51*) and was assessed by template modeling scores (TM-scores). The alignments and trees generated in this study are available at https://figshare.com/s/a403e104930ca9d6e712.

Construction of plasmids and yeast strains

cDNA sequences of *hsPKR*, *pbPKR*, *xtPKR*, *paPKR*, *drPKR*, *rtPKR*, and *scPKR-sis* genes with hemagglutinin (HA) tags at the C termini were synthesized by Genewiz laboratory (Jiangsu, China) (table S3). The codons for *hsPKR*, *pbPKR*, *xtPKR*, *paPKR*, and *rtPKR* genes were optimized (table S4). The expression plasmids of *PKR* genes using the Gal-HF vector were constructed as described previously (*30*). Briefly, *PKR* genes were synthesized and then ligated to the Gal-HF vector via the Seamless Cloning Kit (Beyotime no. D7010M). The expression of *PKR* genes was induced by a galactose-induced promoter (GAL1/10). Full-length *scPKR-sis* and *scPKR-sis-KD* were cloned into the pGEX-4T-2 plasmid to construct a GST-tagged fusion protein. The fusion protein genes were amplified from the pGEX-4T-2 plasmid using polymerase chain reaction (PCR) and then ligated into the GAL expression vector using seamless cloning. Site-specific mutations for *PKR* genes were generated by PCR mutagenesis using Phanta Max Super-Fidelity DNA Polymerase (Vazyme no. P505-d2). Primers with the desired mutations (table S4) were synthesized by Sangon Biotech (Shanghai, China). All the strains used in this study were derived from *S. cerevisiae* laboratory strain S288C. The yeast strain with the eIF2α^{S51A} mutation was generated using CRISPR-Cas9 gene-editing technology. sgRNA (5′-AATTGTCCCGTAGACG-TATT-3′) was designed using CRISPRdirect (*52*). The eIF2α^{S51A} mutation was confirmed by sequencing.

Spot assay

Yeast strains were cultured in yeast extract, peptone, and dextrose (YPD) liquid medium containing G418 (0.5 mg/ml; Sangon, Shanghai, China) at 30°C with shaking at 200 rpm overnight. Yeast strains were then transferred to fresh YPD liquid medium and grown to an optical density at 600 nm (OD_{600}) value of about 3. Cells were harvested by centrifugation, and OD_{600} was adjusted to 3. Tenfold serial dilutions (OD_{600} = 3, 0.3, 0.03, 0.003, and 0.0003) were prepared, followed by spotting 2 μl of each dilution on the surface of solid medium containing 2% glucose or 2% galactose. Imaging was performed after 48 and 72 hours, respectively.

Western blotting

Yeast strains were cultured in selective YPD liquid medium at 30°C with shaking at 200 rpm overnight. Yeast strains incubated overnight were transferred to fresh YPD liquid and grown to the log phase (OD_{600} of about 0.6). Cell pellets were collected by centrifugation and washed twice before being induced by 2% galactose for 6 hours. Then, cell pellets were harvested (~1×10^8 cell) by

centrifugation for protein extraction. Yeast whole-cell extracts were prepared through alkaline extraction (*53*). Briefly, harvested yeast cells were resuspended in 80 μl of lysate (1.8 M NaOH, 10 mM phenylmethanesulfonyl fluoride, and 1% β-mercaptoethanol) and then added by 500 μl of ddH_2O for 5 min to lyse the cells. An equal volume of 50% trichloroacetic acid was added to the above solution to form protein precipitation. Sediments were obtained by centrifugation at 10,000*g* for 5 min at 4°C and subsequently washed in 0.5 M tris-HCl and ultrapure water. The samples were dissolved in 5× protein loading buffer (Abclonal no. RM00001) and boiled for 10 min. Equal protein amounts of cell lysates were electrophoresed on 10% SDS-PAGE and transferred onto a polyvinylidene difluoride membrane (Merck Millipore no. IPVH00010). After blocking with either 5% nonfat dry skim milk or 5% bovine serum albumin for 2 hours at room temperature, the membrane was incubated overnight at 4°C with different antibodies diluted in TBS-T [20 mM tris-HCl (pH 7.6), 150 mM NaCl, and 0.1% Tween 20] in turn [1:5000 for mouse anti-HA (Abclonal no. AE008), 1:5000 for mouse anti-GST (Abclonal no. AE001), 1:5000 for rabbit phospho-eIF2α-S51 (Abclonal no. AP0342), or 1:10,000 for β-actin (Proteintech no. 60008-1-lg)]. After triple washes, membrane was incubated for 1 hour with an IRDye infrared secondary antibody diluted in TBS-T [1:10,000 for goat anti-mouse immunoglobulin G (IgG; LI-COR no. 926-68070), and 1:10,000 for goat anti-rabbit IgG (LI-COR no. 926-68071)]. The blot bands were visualized by the Odyssey Imaging System.

Supplementary Materials

This PDF file includes:

Figs. S1 to S3

Tables S1 to S4

REFERENCES AND NOTES

1. J. Wu, Z. J. Chen, Innate immune sensing and signaling of cytosolic nucleic acids. *Annu. Rev. Immunol.* **32**, 461–488 (2014).
2. M. Schlee, G. Hartmann, Discriminating self from non-self in nucleic acid sensing. *Nat. Rev. Immunol.* **16**, 566–580 (2016).
3. Y. G. Chen, S. Hur, Cellular origins of dsRNA, their recognition and consequences. *Nat. Rev. Mol. Cell Biol.* **23**, 286–301 (2022).
4. D. Levin, I. M. London, Regulation of protein synthesis: Activation by double-stranded RNA of a protein kinase that phosphorylates eukaryotic initiation factor 2. *Proc. Natl. Acad. Sci. U.S.A.* **75**, 1121–1125 (1978).
5. T. E. Dever, Gene-specific regulation by general translation factors. *Cell* **108**, 545–556 (2002).
6. A. C. Dar, T. E. Dever, F. Sicheri, Higher-order substrate recognition of eIF2α by the RNA-dependent protein kinase PKR. *Cell* **122**, 887–900 (2005).
7. S. Rothenburg, E. J. Seo, J. S. Gibbs, T. E. Dever, K. Dittmar, Rapid evolution of protein kinase PKR alters sensitivity to viral inhibitors. *Nat. Struct. Mol. Biol.* **16**, 63–70 (2009).
8. E. Meurs, K. Chong, J. Galabru, N. S. Thomas, I. M. Kerr, B. R. Williams, A. G. Hovanessian, Molecular cloning and characterization of the human double-stranded RNA-activated protein kinase induced by interferon. *Cell* **62**, 379–390 (1990).
9. S. Balachandran, P. C. Roberts, L. E. Brown, H. Truong, A. K. Pattnaik, D. R. Archer, G. N. Barber, Essential role for the dsRNA-dependent protein kinase PKR in innate immunity to viral infection. *Immunity* **13**, 129–141 (2000).
10. D. A. Leib, M. A. Machalek, B. R. Williams, R. H. Silverman, H. W. Virgin, Specific phenotypic restoration of an attenuated virus by knockout of a host resistance gene. *Proc. Natl. Acad. Sci. U.S.A.* **97**, 6097–6101 (2000).
11. D. F. Stojdl, N. Abraham, S. Knowles, R. Marius, A. Brasey, B. D. Lichty, E. G. Brown, N. Sonenberg, J. C. Bell, The murine double-stranded RNA-dependent protein kinase PKR is required for resistance to vesicular stomatitis virus. *J. Virol.* **74**, 9580–9585 (2000).
12. M. D. Daugherty, H. S. Malik, Rules of engagement: Molecular insights from host-virus arms races. *Annu. Rev. Genet.* **46**, 677–700 (2012).
13. L. Quintana-Murci, A. G. Clark, Population genetic tools for dissecting innate immunity in humans. *Nat. Rev. Immunol.* **13**, 280–293 (2013).
14. M. Sironi, R. Cagliani, D. Forni, M. Clerici, Evolutionary insights into host-pathogen interactions from mammalian sequence data. *Nat. Rev. Genet.* **16**, 224–236 (2015).
15. J. O. Langland, J. M. Cameron, M. C. Heck, J. K. Jancovich, B. L. Jacobs, Inhibition of PKR by RNA and DNA viruses. *Virus Res.* **119**, 100–110 (2006).
16. J. O. Langland, B. L. Jacobs, The role of the PKR-inhibitory genes, E3L and K3L, in determining vaccinia virus host range. *Virology* **299**, 133–141 (2002).
17. A. C. Dar, F. Sicheri, X-ray crystal structure and functional analysis of vaccinia virus K3L reveals molecular determinants for PKR subversion and substrate recognition. *Mol. Cell* **10**, 295–305 (2002).
18. N. C. Elde, S. J. Child, A. P. Geballe, H. S. Malik, Protein kinase R reveals an evolutionary model for defeating viral mimicry. *Nature* **457**, 485–489 (2009).
19. S. B. Hedges, J. Marin, M. Suleski, M. Paymer, S. Kumar, Tree of life reveals clock-like speciation and diversification. *Mol. Biol. Evol.* **32**, 835–845 (2015).
20. M. Friedman, Fossils reveal the deep roots of jawed vertebrates. *Nature* **609**, 897–898 (2022).
21. M. Dey, C. Cao, A. C. Dar, T. Tamura, K. Ozato, F. Sicheri, T. E. Dever, Mechanistic link between PKR dimerization, autophosphorylation, and eIF2α substrate recognition. *Cell* **122**, 901–913 (2005).
22. E. J. Seo, F. Liu, M. Kawagishi-Kobayashi, T. L. Ung, C. Cao, A. C. Dar, F. Sicheri, T. E. Dever, Protein kinase PKR mutants resistant to the poxvirus pseudosubstrate K3L protein. *Proc. Natl. Acad. Sci. U.S.A.* **105**, 16894–16899 (2008).
23. T. E. Dever, J. J. Chen, G. N. Barber, A. M. Cigan, L. Feng, T. F. Donahue, I. M. London, M. G. Katze, A. G. Hinnebusch, Mammalian eukaryotic initiation factor 2 alpha kinases functionally substitute for GCN2 protein kinase in the GCN4 translational control mechanism of yeast. *Proc. Natl. Acad. Sci. U.S.A.* **90**, 4616–4620 (1993).
24. C. M. Carey, A. A. Govande, J. M. Cooper, M. K. Hartley, P. J. Kranzusch, N. C. Elde, Recurrent loss-of-function mutations reveal costs to OAS1 antiviral activity in primates. *Cell Host Microbe* **25**, 336–343.e4 (2019).
25. L. G. Ortega, M. D. McCotter, G. L. Henry, S. J. McCormack, D. C. Thomis, C. E. Samuel, Mechanism of interferon action. *Virology* **215**, 31–39 (1996).
26. S. Rothenburg, N. Deigendesch, K. Dittmar, F. Koch-Nolte, F. Haag, K. Lowenhaupt, A. Rich, A PKR-like eukaryotic initiation factor 2α kinase from zebrafish contains Z-DNA binding domains instead of dsRNA binding domains. *Proc. Natl. Acad. Sci. U.S.A.* **102**, 1602–1607 (2005).
27. C. Y. Hu, Y. B. Zhang, G. P. Huang, Q. Y. Zhang, J. F. Gui, Molecular cloning and characterisation of a fish PKR-like gene from cultured CAB cells induced by UV-inactivated virus. *Fish Shellfish Immunol.* **17**, 353–366 (2004).
28. C. Wu, Y. Zhang, C. Hu, PKZ, a fish-unique eIF2α kinase involved in innate immune response. *Front. Immunol.* **11**, 585 (2020).
29. Z. Gong, J. Qi, M. Hu, G. Bi, J. M. Zhou, G. Z. Han, The origin and evolution of a plant resistosome. *Plant Cell* **34**, 1600–1620 (2022).
30. L. Chu, Z. Gong, W. Wang, G. Z. Han, Origin of the OAS-RNase L innate immune pathway before the rise of jawed vertebrates via molecular tinkering. *Proc. Natl. Acad. Sci. U.S.A.* **120**, e2304687120 (2023).
31. C. J. Bierle, K. M. Semmens, A. P. Geballe, Double-stranded RNA binding by the human cytomegalovirus PKR antagonist TRS1. *Virology* **442**, 28–37 (2013).
32. G. W. Litman, J. P. Rast, S. D. Fugmann, The origins of vertebrate adaptive immunity. *Nat. Rev. Immunol.* **10**, 543–553 (2010).
33. S. Huang, X. Tao, S. Yuan, Y. Zhang, P. Li, H. A. Beilinson, Y. Zhang, W. Yu, P. Pontarotti, H. Escriva, Y. Le Petillon, X. Liu, S. Chen, D. G. Schatz, A. Xu, Discovery of an active RAG transposon illuminates the origins of V(D)J recombination. *Cell* **166**, 102–114 (2016).
34. M. F. Flajnik, A cold-blooded view of adaptive immunity. *Nat. Rev. Immunol.* **18**, 438–453 (2018).
35. T. Wein, R. Sorek, Bacterial origins of human cell-autonomous innate immune mechanisms. *Nat. Rev. Immunol.* **22**, 629–638 (2022).
36. F. Leulier, B. Lemaitre, Toll-like receptors—Taking an evolutionary approach. *Nat. Rev. Genet.* **9**, 165–178 (2008).
37. J. J. Brennan, T. D. Gilmore, Evolutionary origins of Toll-like receptor signaling. *Mol. Biol. Evol.* **35**, 1576–1587 (2018).
38. G. Ofir, E. Herbst, M. Baroz, D. Cohen, A. Millman, S. Doron, N. Tal, D. B. A. Malheiro, S. Malitsky, G. Amitai, R. Sorek, Antiviral activity of bacterial TIR domains via immune signalling molecules. *Nature* **600**, 116–120 (2021).
39. Y. Li, K. M. Slavik, H. C. Toyoda, B. R. Morehouse, C. C. de Oliveira Mann, A. Elek, S. Levy, Z. Wang, K. S. Mears, J. Liu, D. Kashin, X. Guo, T. Mass, A. Sebé-Pedrós, F. Schwede, P. J. Kranzusch, cGLRs are a diverse family of pattern recognition receptors in innate immunity. *Cell* **186**, 3261–3276.e20 (2023).
40. E. M. Culbertson, T. C. Levin, Eukaryotic antiviral immune proteins arose via convergence, horizontal transfer, and ancient inheritance. bioRxiv [Preprint] (2023); https://doi.org/10.1371/journal.pbio.3002436.
41. B. R. Morehouse, A. A. Govande, A. Millman, A. F. A. Keszei, B. Lowey, G. Ofir, S. Shao, R. Sorek, P. J. Kranzusch, STING cyclic dinucleotide sensing originated in bacteria. *Nature* **586**, 429–433 (2020).

42. A. S. Gizzi, T. L. Grove, J. J. Arnold, J. Jose, R. K. Jangra, S. J. Garforth, Q. Du, S. M. Cahill, N. G. Dulyaninova, J. D. Love, K. Chandran, A. R. Bresnick, C. E. Cameron, S. C. Almo, A naturally occurring antiviral ribonucleotide encoded by the human genome. *Nature* **558**, 610–614 (2018).
43. A. Bernheim, A. Millman, G. Ofir, G. Meitav, C. Avraham, H. Shomar, M. M. Rosenberg, N. Tal, S. Melamed, G. Amitai, R. Sorek, Prokaryotic viperins produce diverse antiviral molecules. *Nature* **589**, 120–124 (2021).
44. S. R. Eddy, Accelerated profile HMM searches. *PLoS Comput. Biol.* **7**, e1002195 (2011).
45. K. Katoh, D. M. Standley, MAFFT multiple sequence alignment software version 7: Improvements in performance and usability. *Mol. Biol. Evol.* **30**, 772–780 (2013).
46. M. N. Price, P. S. Dehal, A. P. Arkin, FastTree 2—Approximately maximum-likelihood trees for large alignments. *PLOS ONE* **5**, e9490 (2010).
47. L. T. Nguyen, H. A. Schmidt, A. von Haeseler, B. Q. Minh, IQ-TREE: A fast and effective stochastic algorithm for estimating maximum-likelihood phylogenies. *Mol. Biol. Evol.* **32**, 268–274 (2015).
48. A. Marchler-Bauer, M. K. Derbyshire, N. R. Gonzales, S. Lu, F. Chitsaz, L. Y. Geer, R. C. Geer, J. He, M. Gwadz, D. I. Hurwitz, C. J. Lanczycki, F. Lu, G. H. Marchler, J. S. Song, N. Thanki, Z. Wang, R. A. Yamashita, D. Zhang, C. Zheng, S. H. Bryant, CDD: NCBI's conserved domain database. *Nucleic Acids Res.* **43**, D222–D226 (2015).
49. M. Mirdita, K. Schütze, Y. Moriwaki, L. Heo, S. Ovchinnikov, M. Steinegger, ColabFold: Making protein folding accessible to all. *Nat. Methods* **19**, 679–682 (2022).
50. M. Varadi, S. Anyango, M. Deshpande, S. Nair, C. Natassia, G. Yordanova, D. Yuan, O. Stroe, G. Wood, A. Laydon, A. Žídek, T. Green, K. Tunyasuvunakool, S. Petersen, J. Jumper, E. Clancy, R. Green, A. Vora, M. Lutfi, M. Figurnov, A. Cowie, N. Hobbs, P. Kohli, G. Kleywegt, E. Birney, D. Hassabis, S. Velankar, AlphaFold protein structure database: Massively expanding the structural coverage of protein-sequence space with high-accuracy models. *Nucleic Acids Res.* **50**, D439–D444 (2022).
51. H. M. Berman, J. Westbrook, Z. Feng, G. Gilliland, T. N. Bhat, H. Weissig, I. N. Shindyalov, P. E. Bourne, The Protein Data Bank. *Nucleic Acids Res.* **28**, 235–242 (2000).
52. Y. Naito, K. Hino, H. Bono, K. Ui-Tei, CRISPRdirect: Software for designing CRISPR/Cas guide RNA with reduced off-target sites. *Bioinformatics* **31**, 1120–1123 (2015).
53. Y. Matsuo, K. Asakawa, T. Toda, S. Katayama, A rapid method for protein extraction from fission yeast. *Biosci. Biotech. Bioch.* **70**, 1992–1994 (2006).

Acknowledgments

Funding: This work was supported by National Natural Science Foundation of China (32300511 and 32270684). **Author contributions:** Conceptualization: G.-Z.H. Investigation: Z.W., L.C., and Z.G. Supervision: G.-Z.H. Writing–original draft: G.-Z.H. Writing–review and editing: Z.W., L.C., and Z.G. **Competing interests:** The authors declare that they have no competing interests. **Data and materials availability:** All data needed to evaluate the conclusions in the paper are present in the paper and/or the Supplementary Materials.

Submitted 19 February 2024
Accepted 28 June 2024
Published 7 August 2024
10.1126/sciadv.ado7464